Shahrood University of Technology
Iranian Society of Mining Engineering (IRSME)
Journal of Mining and Environment (JME)
journal homepage: www.jme.shahroodut.ac.ir
THOMSON REUTERS

Challenges for In-Situ Stress Measurement in Rock Caverns by Hydraulic Fracturing and HTPF Tests-Case Study: Azad Hydropower Project

Mohammad Reza Shahverdiloo* and Shokroallah Zare

Faculty of Mining, Petroleum and Geophysics Engineering, Shahrood University of Technology, Shahrood, Iran

Article Info

Received 18 April 2021
Received in Revised form 1 June 2021
Accepted 7 June 2021
Published online 7 June 2021

DOI:10.22044/jme.2021.10673.2037

Keywords

Stress Measurement
Stress State
Hydraulic Fracturing
HTPF
Heterogeneity

Abstract

Hydraulic fracturing (HF) and hydraulic testing of pre-existing fractures (HTPF) are efficient hydraulic methods in order to determine the in-situ stress of rock mass. Generally, the minimum (Sh) and maximum (SH) horizontal principal stresses are measured by hydraulic methods; the vertical stress (SV) is calculated by the weight of the overburden layers. In this work, 37 HF and HTPF tests are conducted in a meta-sandstone, which has about 10% inter-layer phyllite. The artesian circumstance, considerable gap between the drilling and hydraulic tests in the long borehole, no underground access tunnel to rock cavern at the early stages of projects, and a simplified hypothesis theory of HF are the main challenges and limitations of the HF/HTPF measurements. Due to the instability in the long borehole, the drill rig type and borehole length are revised; also TV logger is added to the process of selection of the test's deep. The HF/HTPF data is sequentially analyzed by the classic and inversion methods in order to achieve an optimum number of hydraulic tests. Besides, The SH magnitude in the inversion method is lower than the classic method; the relevant geological data and the faulting plan analysis lead to validate the SH and Sh magnitudes and the azimuths obtained by the classic method. The measured SH and Sh magnitudes are 7-17 MPa and 4-11 MPa, respectively; the calculated vertical stress magnitude is 6-14 MPa at the test locations. Indeed, the stress state is (SH > SV > Sh), and SH azimuth range is 56-93 degrees.

1. Introduction

The in-situ stress state in the earth's crust is a considerable important concept in many problems dealing with rocks in the civil, mining, well bore mechanics and the reservoir engineering operations as well as geology and geophysics (Amadei and Stephansson, 1997) [2]. The in-situ stress information may be required for the following rock engineering aspects, either directly or as an input factor to the analytical analyses or numerical models:

- temporary or permanent stability of underground spaces, e.g. tunnels, caverns, shafts, and other openings (Ji and Guo, 2020; Li et al., 2017) [24; 30];
- assessment of the efficient excavation methods (drill-and-blast or TBM);
- design of the supporting systems of rocks (Shahverdiloo et al., 2014; Alemdag et al., 2019) [43; 3];
- design of lining of waterway system in hydropower project (Shahverdiloo, 2010) [42];
- prediction of rock bursts (Miao et al., 2016) [35];
- thermo-hydro-mechanical behavior of the rock (Huan et al., 2021) [19];
- design of grout methodology (Liu et al., 2019) [31];
- fluid flow and contaminant transport (Mortimer et al., 2011) [36];
- Fracturing and fracture propagations (Bakhshi et al., 2019; Abdollahipour et al., 2016) [5; 1].

Corresponding author: mr.shahverdiloo@shahroodut.ac.ir (M.R. Shahverdiloo).

Obtaining reliable estimates of the stress tensor, which can be estimated by measuring or calculation of the pressure in different directions inside a rock mass, is a challenging task due to the very nature of the concept "stress" and due to the practical reasons. The quantitative evaluation of the principal horizontal in-situ stresses, i.e. maximum (SH) and minimum (Sh), at a specific site cannot be made since the gravitational/vertical stress (SV) is practically the only one clearly understood. Hence, these horizontal stresses require direct measurements in the field. The in-situ stress measurement methods, e.g. hydraulic fracturing (HF), hydraulic testing of the pre-existing fractures (HTPF), dilatometer, and over-coring approaches, have been developed based on the elastic materials in order to determine the original stress state. Under specific geological conditions and the project's limitations, some methods have a significant advantage over the others. However, Due to the variability inherent to the in-situ stress measurement and the role of scale effect, i.e. effects of discontinuity and heterogeneity, a main query is how many measurements are required to obtain the mean in-situ stress estimates of an acceptable reliability (Feng et al., 2019) [11].

Hydraulic fracturing was initially used for the reservoir productivity stimulation, and was applied to stress measurement in the early 1960s. Hung et al. (2009) [23] have successfully conducted this measurement below a 1 km depth. Currently, there are two major categories including the conventional hydraulic fracturing (HF) and hydraulic tests on the pre-existing fractures (HTPF). HF is now a well-established technique for determining the in-situ stresses at depth (Hubbert and Willis, 1957; Scheidegger, 1960; Kehle, 1964; Haimson and Fairhurst, 1969, 1970; Zoback and Haimson, 1982; Haimson, 1989; Serata et al. 1992; Haimson and Cornet, 2003; Sano et al., 2005) [20; 41; 25; 14; 15; 47; 16; 40; 17; 39]. The main advantages of the HF test are performing in an existing hole, low scattering in the results, involving a fairly large rock volume, and being quick; in contrast, the only 2D, the theoretical weakness in the evaluation of major horizontal stress (SH), and disturbance of water chemistry are its limitations. The significant advantage of the HTPF test is its applicability in the high stress rocks in which over-coring and HF fails; on the other hand, time-consumption, requiring the existing fractures in the hole with varying strikes, and dips are the main limitations of the HTPF test. Rutqvist et al., (2000) [38] have mentioned that the general theory for SH calculation from hydraulic fracturing suffers from the uncertainties in the assumptions of continuous, linearly elastic, homogenous, and isotropic rocks together with fracture re-opening. However, due to some uncertainties such as plastic behaviors of the surrounding rock (Rutqvist et al., 2000) [38] and the remaining apertures at the start of each cycle (Cornet, 1993) [9] measurement of the re-opening pressure may not be accurate. Lakirouhani et al. (2016) [28] believed that near-wellbore stress state should be taken into account; the compressibility of the injection system and the viscous flow of water can diminish the accuracy of the stress estimates; these issues have not been well-quantified. Krietsch et al. (2017) [27] have reported that the survey combines over-coring with hydro-fracture measurements with concomitant monitoring of the induced micro-seismicity, in which the use of a transversely isotropic model for inverting the strains measured during over-coring is essential to obtain stress solutions that are consistent with the hydro-fracture and micro-seismicity results. The utilization of the micro-seismic monitoring system (Xiao et al., 2016) [45] and the acoustic emission technique (Lan et al., 2011; Bai, 2018) [29; 6] have been developed for the HF mapping and Kiser effects, respectively.

Unanimously, the reliability of rock stress measurements is partly dependent on the measuring technique and equipment, and partly dependent on the nature of rock masses. This work focuses on the hydraulic methods with an emphasis on the equipment and rock mass challenges involved in the deepest hydropower complex caverns in Iran.

2. Hydraulic methods

There exist two stress measurement approaches, i.e. HF and HTPF, in which the water pressure is used to stimulate the rock surrounding a borehole, and hence, to determine the in-situ stress state. Both approaches use quite similar equipment, including straddle packers, impression packer, and special pumps to generate high-pressure water to make a new fracture or re-opening of the pre-existing fractures (Ljunggren et al., 2003) [32]. Pressure is applied into the test chamber, which is isolated by straddle packers, until a new fracture is created (Figure 1) or the existing fracture is opened (Figure 2) (Amadei and Stephansson, 1997) [2].

The classical HF theory requires isotropic, elastic, homogeneous, and impermeable rock materials at a depth subjected to three principal stresses (Hubbert and Willis, 1957) [20]. HF provides a simple way to measure stress magnitudes; advance knowledge of rock properties, e.g. Young′s modulus and Poisson′s ratio, is not fundamental. The HF test procedure comprises of (a) pressurization of the selected test chamber until fracturing occurs, and (b) delineation of the induced fracture. Typically, a complete test consists of two trips down-hole to the test interval, each with different equipment assemblies. The straddle packer system is the most common tool for fracturing; the oldest and still the most reliable fracture tracing on the borehole wall is the impression-orienting tool (Figure 1). Generally, one principal stress is assumed to be parallel to the axis of a vertical borehole, SV, and equals the gravitational stress of the material above the specified depth, i.e. SV = ρgz, where ρ is the rock mass density in kg/m3; g is the ground acceleration, 9.81 m/s2; and z is the overburden in m (Zang and Stephansson, 2009) [46]. Figure 1 shows the HF test's essential factors including the breakdown or cracking pressure (Pc) and the shut-in pressure (Psi). The Sh value is equal to Psi, and SH is calculated by Eq. (1).

$$S_H = 3 \times S_h - P_r - P_o \quad (1)$$

where P_0 is the pore pressure, and Pr is the re-opening pressure.

The HTPF test was initially proposed by Cornet and Valette (1984) [7], and was designed to overcome the shortcomings of the HF method. Compared with the HF method, HTPF focuses on the re-opening of the pre-existing fracture in the sealed section (Figure 2). This technique aims to determine the normal stresses acting perpendicular to the pre-existing fractures, which equal to the shut-in pressure generated by fluid injection. Accordingly, it is vital to gather the precise locations and the orientations of fractures before the commencement of the fluid injection. This is usually achieved by the borehole imaging techniques, like the Mosnier tool (Cornet *et al*., 2003) [10]. Theoretically, the 2D solution requires at least six different fractures to solve the problem. In practice, however, some redundancy is required. For successful measurements, it is suggested that at least 10–12 isolated, pre-existing fractures with different dips and dip-directions are found and tested in the borehole wall within the depth interval of interest. The 3D alternative of the HTPF method includes fewer assumptions on the stress state but requires a more significant number of fractures to be tested. In the 3D option, SV does not have to be a principal stress. Hypothetically, 12 unknowns exist in the system of equations. Practically, it is recommended that at least 18–20 successful tests are obtained to resolve the 3D in-situ stress state (Ljunggren, 2003) [32].

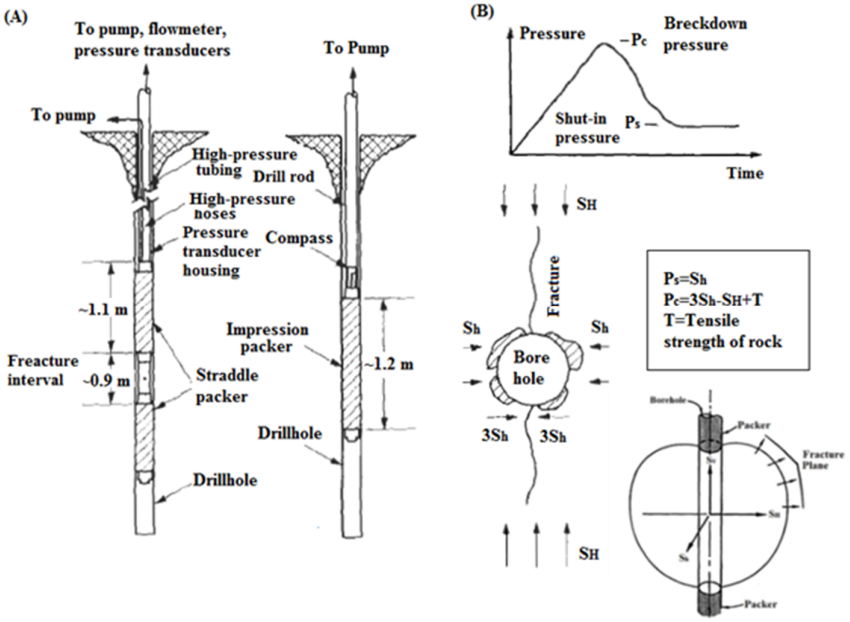

Figure 1. (A) Hydraulic fracturing system (B) Associated calculations (Kim and Franklin, 1987) [26].

The HTPF main limitations are caused by (a) the hypothesis that the fractures observed at the wellbore remain planar in the domain investigated by the hydraulic methods; (b) the assumptions concerning the regional stress field variation within the domain of interest; and (c) the considerable number of tests required if the solution is to be well-constrained.

3. Rock cavern hydraulic tests

3.1. Site description

The Azad pumped-storage power plant (PSPP) is located in the western region of Iran consisting of a complex relatively deep overburden of about 466 m caverns, and a long vertical pressure shaft (Figure 3). The mentioned underground spaces are located in a zone of meta-sandstone with about 10% inter-layer phyllite; the mean rock mass unite weight is 27100 N/m3 (*RMRA* and EGRA, 2013) [33; 34].

Due to lack of access tunnel to caverns, the execution progress dictated the long boreholes (AP2 and AP3) for the HF/HTPF tests that were drilled from an access tunnel (IAT) about 250 m above the complex cavern elevation (Figures. 3 and 4). The first phase of the HF/HTPF tests failed after 2+7 tests due to a borehole collapse, i.e. the straddle packer was trapped at the AP3 borehole, and the possibility of trapping the second straddle packer in the AP2 borehole. Then the second phase of the HF/HTPF tests was conducted in an intermediate borehole length (HF1, HF2, and HF3) at the T1 access tunnel (Figures 3 and 4). In brief, the in-situ stress measurements consisted of two phases in which 37 HF/HTPF tests were conducted in four different periods in vertical boreholes.

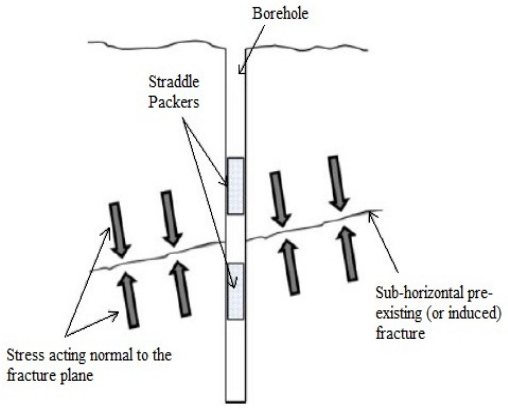

Figure 2. Schematic view of HTPF (Gaines et al., 2012) [13].

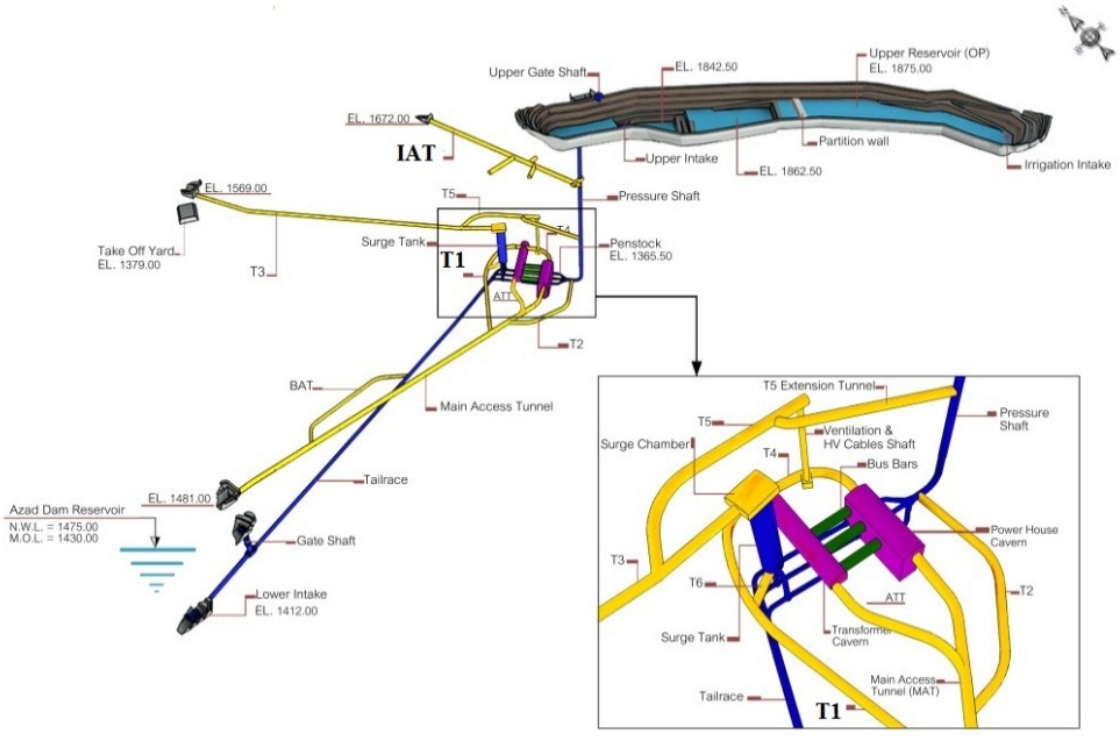

Figure 3. 3D layout of Azad PSPP.

The groundwater table (GWT) is about 1640 and 1390 m.a.s.l (meters above the sea level) in the first and second phases, respectively (Figure 4). The rock is generally impermeable (lugeon < 5) but the limited fracture zones have a high permeability (lugeon > 60) (EGRA, 2013) [34].

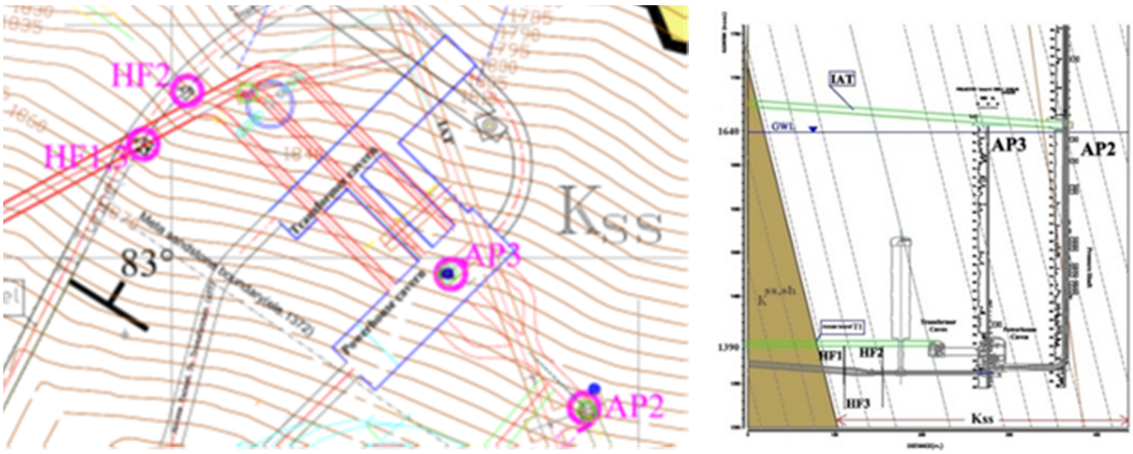

Figure 4. HF/HTPF borehole profile, AP 2 and 3 and HF 1 and 2 and 3, Left plan Right longitudinal (EGRA, 2013) [34].

3.2. HF/HTPF first phase

The first phase of the HF/HTPF test was performed in the AP 2 and 3 boreholes, which were vertically drilled from the intermediate access tunnel (IAT) toward the complex caverns (Figure 4). These boreholes belonging to the exploratory borehole series were dictated for the complementing of the site investigation plan (Table 1).

Table 1. Specification of the AP 2 and 3 borehole (EGRA, 2013) [34].

Borehole	Drilling rig	Type	Diameter (mm)	Coring date		Top elevation (m)	Over-burden (m)	Length (m)
				Start	Finish	z		
Ap2	DB850	Wireline	96	March 2013	December 2013	1642	233	285
Ap3	Longyear	Conventional	101-76	December 2012	June 2013	1645	215	300

Initially, the depth of the hydraulic test was selected by the rock core assessment. The HF/HTPF tests began at the deepest test location in Ap3, the borehole length (BL) 294.5 m, but after the second test, BL 287.5 m, the straddle packer was trapped at a depth of 260 m. All the efforts were unsuccessful in releasing the straddle packer set, i.e. the straddle packer was buried. Therefore, the impression packer could not determine the fracture/joint orientation in the mentioned tests. It seems that the drilling rig system, which can apply a huge upward or downward force, is the better choice against the sturdy tripod system, which is a rapid transferring system with only an upward force, for releasing the trapped straddle packer.

The borehole TV inspection revealed an unexpected condition, collapse zone, in the borehole circumference. Although the core samples visually had a good situation, the TV logger was recorded inconsistently with them; the more irregular borehole circumference is shown in Figure 5. The preliminary investigation for the mentioned situation led to the following options: improving the drilling rig type, minimizing the gap between borehole drilling and hydraulic testing, and involving the TV inspection for selecting the HF/HTPF test depth. The relatively soft rock, i.e. phyllite inter-layer or calcite infilling, in the hard rock, i.e. meta-sandstone, may be the leading cause of irregularity of the borehole wall and consequently instability.

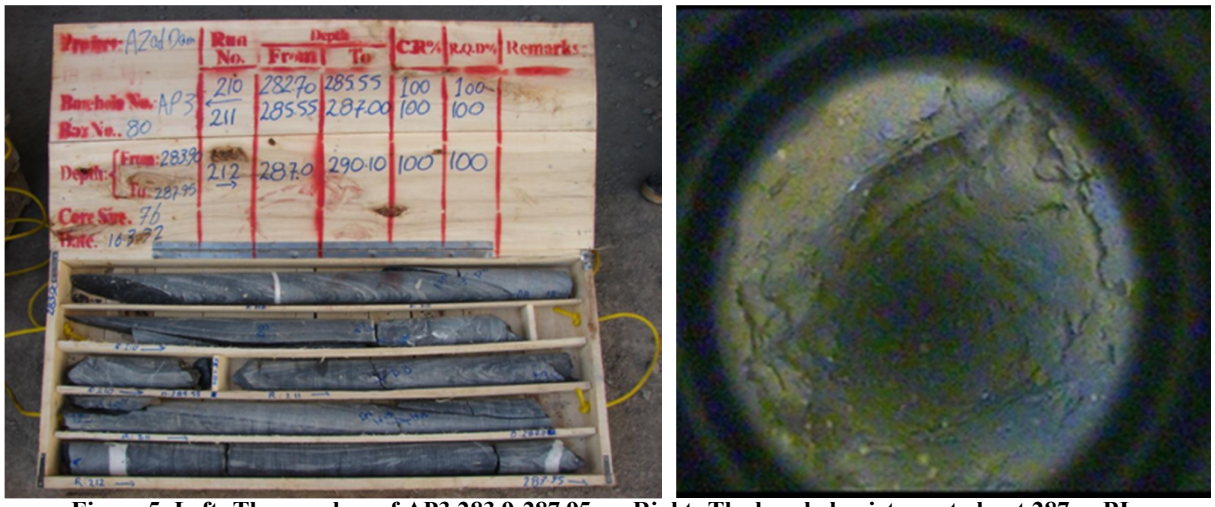

Figure 5. Left: The core box of AP3 283.9-287.95 m; Right: The borehole picture at about 287 m BL.

The sequences of the HF/HTPF process in AP2 was revised; first of all, the TV borehole inspection was a prerequisite to finalizing the HF/HTPF test location; secondly, the drilling rig type was changed from the conventional to the wireline method. The wireline core barrel allows drilling or coring without pulling the drill string; thirdly, the gap between the borehole drilling and the HF/HTPF test was minimized by the sequential drilling section up to 100 m. The mentioned revisions made the situation better but there was another straddle packer loss challenge beyond 70 m BL; because a fractured zone appeared in the borehole, and there was a possibility of another straddle packer losing. Consequently, only seven HF/HTPF tests were performed in 70 out of 285 m of AP2 BL. In brief, the first phase has had only 9 HF/HTPF tests. Due to the limited tests, as mentioned in Sec. 2, the inversion method could not determine the in-situ stress tensor (Hudson, 1995) [22]. Based on the limited HF test, the stress regime was determined as SH > SV > Sh, but the acceptable mean in-situ stress state faced the challenge of insufficient data, and therefore, the continuation of the HF/HTPF test was postponed to the second phase.

3.3. HF/HTPF second phase

Due to the excavation progress, the access tunnels (Figures. 3 and 4) reached the Kss zone, i.e. the meta-sandstone around the complex caverns, then the groundwater level gradually decreased from 1640 to 1390 m.a.s.l over several months (Figure 4). Therefore, the second phase of the HF/HTPF test was performed in the HF series boreholes (Table 2) as close as possible to the complex caverns.

Table 2. Specification of the HF borehole series for HF/HTPF tests (EGRA, 2013) [34].

Borehole	Rig	Type	Diameter (mm)	Coring date		Top elevation (m)	Overburden (m)	Length (m)
				Start	Finish	z		
HF1	Longyear	Conventional	101	September 2014		1393	456	70
HF2				Sep., 14	Oct., 14		438	72
HF3				Dec., 14	Jan., 15		456	45.3

The step-by-step process was the strategy in the second phase, which meant drilling a borehole, conducting the HF/HTPF test, data processing, and analysis until reaching a sufficient number of data test to achieve a reliable in-situ stress. Consequently, the second phase of the in-situ stress measurement was conducted in two stages (Table 3).

4. HF/HTPF test procedure

The HF/HTPF tests were performed in close agreement with the ISRM (International Society of Rock Mechanics) and ASTM (Amadei and Stephansson, 1997; Haimson and Cornet, 2003) [2; 17]. The main apparatus of the HF/HTPF tests are mentioned in Sec.2; the remaining equipment

consists of high-pressure tubing, drill pipe or hose, pressure gauges, pressure transducers, flow-meter, pressure generators, recording equipment, and fracture orientation detection devices (Haimson and Cornet, 2003) [17]. The supply pressure of the hydraulic part of the HF/HTPF equipment was 500 bars, and its flow rate (clean water) was 16 L per min. The control panel system was located near the borehole head in the test station; the measuring sensors were just above the straddle packer (Figure 6). The data acquisition system was set to 8 readings per second; the pressure and flow rate data was recorded during the test execution.

The depth finder, water injection volume, and pressure sensors must be checked and calibrated before each test series. Then, the system operation was simulated by testing the straddle packer in a test pipe (116 mm diameter) for verification of the system operation. Then the straddle packer was sent to the deepest test location of the borehole; the packers were pressurized, and the mentioned pressure usually remains 20 bars more than the pressure in the packed off zone, i.e. pressurized chamber, of the borehole. If the HF/HTPF test process was successful, the straddle packer would be release to remove to the next (upper) test location.

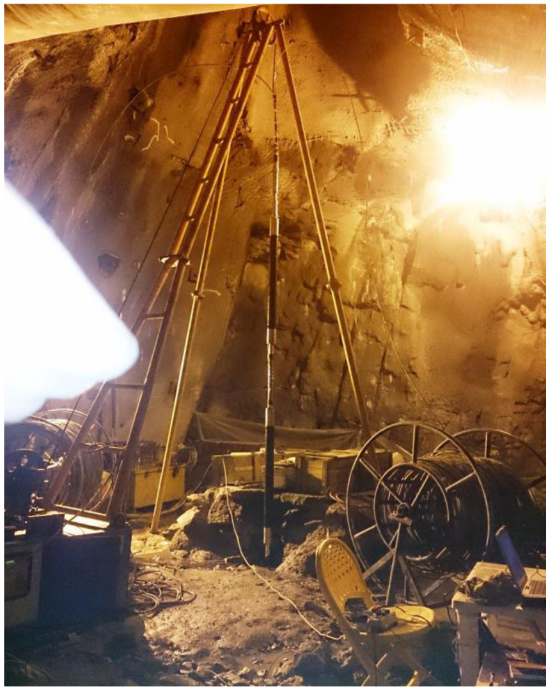

Figure 6. HF/HTPF test station at the top of the HF1 borehole.

The procedures of the HF and HTPF tests have some similarities and differences. The HF test consists of an evaluation of permeability (P-test), rock mass pressurize to induced fracture (Frac. stage), re-opening this fracture (1. Refrac), repeated one or two re-opening stage fracture (2. Refrac. and 3. Refrac.), and finally, one or two step-rate pressurizing (SP/SR). Figure 7 shows the pressure and flow rate of the test chamber versus time according to the mentioned sequences.

Furthermore, the HTPF procedure consists of the evaluation permeability (P-test), the rock mass pressurize to open the existing fracture (Refrac-1), and two step-rate pressurizing stages (1^{st} SP/SR and 2^{st} SP/SR); Figure 8 shows the pressure and flow rate of the test chamber versus time according to the mentioned sequences (GK, 2015) [12].

After all HF/HTPF tests in each borehole, the straddle packer is replaced with an impression packer. The impression packer impressed the discontinuity, i.e. the pre-existing joints or induced fracture, of the HF/HTPF test chamber with a rubber shell covering the packer. The digital compass was applied to precisely record the azimuth and inclination (tilt) of the fracture or pre-existing joint (Figure 9).

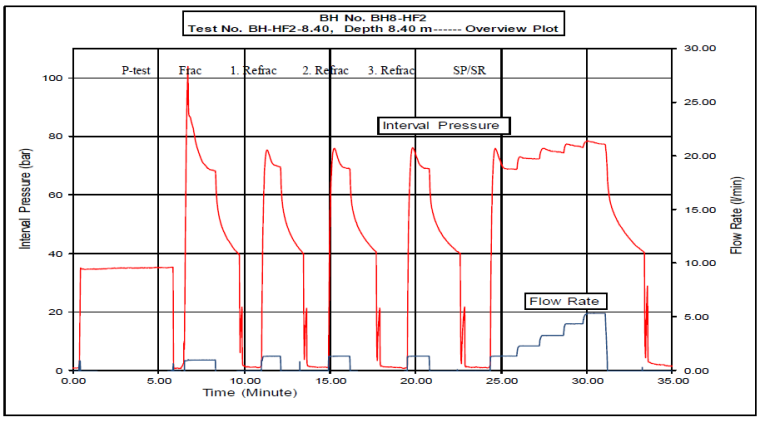

Figure 7. Internal pressure and flow rate *vs.* time curves of the HF test in HF2 borehole- 8.4 m BL (GK, 2015) [12].

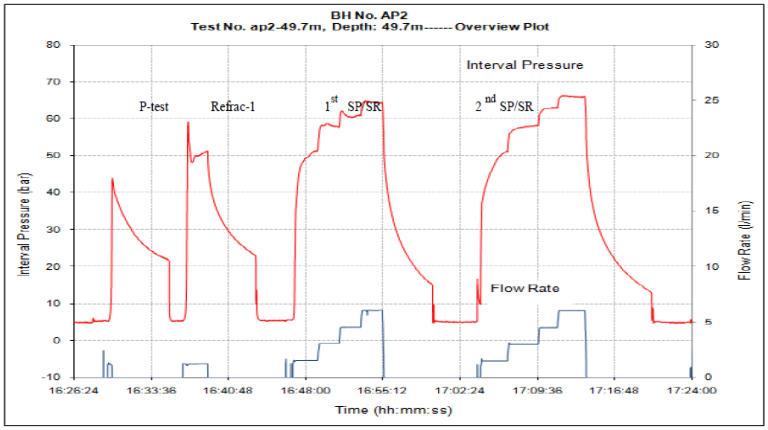

Figure 8. Internal pressure and flow rate *vs.* time curves of the HTPF test in AP2 borehole-49.7 m BL (GK, 2015) [12].

Figure 9. Left: Impression packer; Right: readout unit of the digital compass (GK, 2015) [12].

The impression packer was pressurized higher than the relevant re-opening pressure and held for 30 min under pressure at each test location. After tracing discontinuity on the rubber shell covering the packer (Figure 10), it was replaced with another rubber and repeated for the HF/HTPF test chamber.

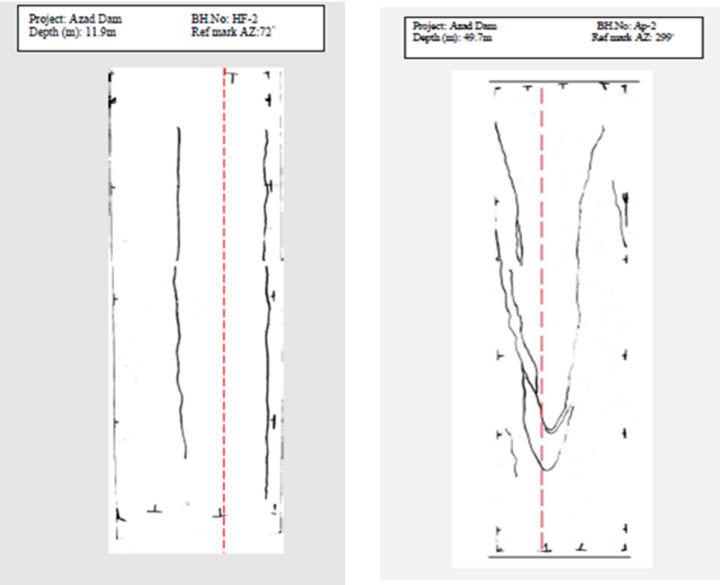

Figure 10. Left: Transparent sheet image display induced fracture trace; Right: Transparent sheet image display pre-existing joint trace (GK, 2015) [12].

5. HF/HTPF test results and discussion

As mentioned in Sec. 2, Pc, Pr, and Psi are the key factors of the HF test. If the pore pressure is negligible, the in-situ hydraulic tensile strength (Pco) will be equal to (Pc-Pr); where Pc is the highest pressure, i.e. the failure pressure; Pr is the pressure of the joint/fracture opening in the first cycle; Psi-max is the pressure at the moment of the closing flow valve (Q = 0) in the pressure-flow curve; Pco is the difference in the failure-reopening pressures, and Psi-min is the pressure at the moment of the deviation of the pressure-time curve from the linear trend was determined by the Muskat method. The shut-in pressure in the HF test was determined by the tangential method (in the third re-opening cycle) as well as in the step rate cycle; however, in the HTPF test, it was determined from the first cycle of opening, and also the first and second step rate cycles. The minimum and maximum shut-in pressures were determined by the Muskat method and tangent method, respectively, which were applied to the pressure-time curve in the position of maximum pressure point, as shown in Figure 11.

The key factors of all the HF/HTPF tests are presented in Table 3. 34 test locations were traced by the impression packer; except AP3-278.5, AP3-294.5, and AP2-65.15 tests. According to the AP series water injection test report, the rock permeability value was about 3 to 5 lugeon. Consequently, the water pore pressure was set to zero in the data analysis (EGRA, 2013) [34]. The calculated Sh value, which is equal to the '3rd refract' column in the mentioned table, is in the range of 4-11 MPa; the SH magnitude, which is calculated by (3×Sh-Pco), is in the range of 7-17 MPa. Besides, the SV magnitude is between 6 and 14 MPa at different test locations.

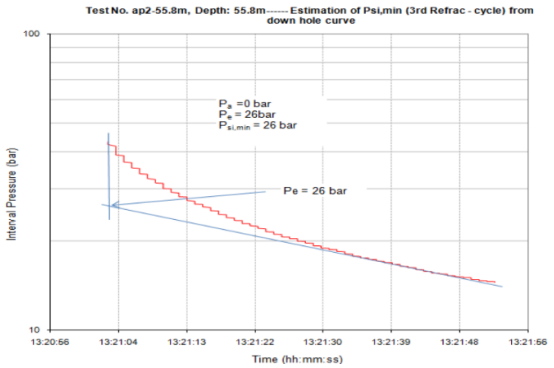

Figure 11. Measurement of Psi in AP2 borehole-55.8 m BL by the Muskat method (GK, 2015) [12].

Generally, Pco is expected to be almost constant. However, there is a noticeable difference in some HF tests (see Table 3), which emphasizes on the hypothesis of cracking welded discontinuity by calcite fillers instead of the virgin rock mass.

Table 3. HF/HTPF test data (GK, 2015) [12].

Phase	Borehole (m)	Type	Depth(m)	Pc-(bar)	Pr-(bar)	Pco-(bar)	Psi(max-(bar)	Psi(min)-(bar)	Psi(bar)				Fracture Strike	Dip Direction	Dip	Date	Stage
									1refrac	3refrac	1SP/SR	2SP/SR					
First	Ap3	HF	287.5	110.5	57	53.5	51	42		49	55					06/21/2013	1
			294.5	250	140	110	145	77		110	94					06/21/2013	
	Ap2	HTPF	22		38		47	35	43		43	43	49	139	75	07/20/2013	2
			29		49		61	45	52		48	48	42	312	70	07/20/2013	
			49.7		34		50	43	48		50	52	20	290	84	07/20/2013	
			54		45		62	53	60		60	62	122	32	69	07/19/2013	
		HF	55.8	70.8	37	33.8	41	26		37	34		29		90	07/19/2013	
		HTPF	62		62		64	62		63	58		112	22	80	07/19/2013	
			65.15													07/19/2013	
Second	HF1	HF	27.2	70	25	45	51.8	44.54		51.27	56.18		144		90	08/10/2014	3
			30.8	66.39	26.8	39.59	57.35	55.18		56.88	65.56		62	332	74	08/10/2014	
			33.5	118.5	72.8	45.65	83.5	72.76		78.76	78.34		357	267	75	08/9/2014	
			35.2	96.36	46.71	49.65	76.5	69.83		75.1	69.8		104	14	68	08/9/2014	
		HTPF	53.2										207	117	39	08/9/2014	
			59.5		64.65		56.81	36.45	54.4		51.8	50	262	352	79	08/9/2014	
			63.5		67.76		78.18	34.35	65		50	51.05	19		90	08/8/2014	
			65.5		73.57		93.28	56.31		76.37	81.46		61	331	79	08/8/2014	
			67.5		66.15		74.28	54.62	73.4		74	89.79	302	212	81	08/7/2014	
	HF2	HF	8.4	103.9	42.52	61.35	67.7	52.17		65	74.92		55	325	78.5	02/11/2015	4
		HTPF	10.4		32.5		53.4	38.67	49.8		49.07	50	147	237	72.5	02/10/2015	
		HF	11.9	71.58	31.28	40.3	61.75	56.53		61.05	64.02		133		90	02/10/2015	
			16.85	10.3.05	62.35	40.7	85.5	79.9		84.7	82.5		77	347	55	02/10/2015	
		HTPF	28.15		42.5		81.93	72.01	80		75	75	82	352	75	02/10/2015	
			32.2		36.52		56	51.8	55.8		75	78.78	233	323	79	02/10/2015	
		HF	33.2	120.1	73.28	46.86	69.34	64.9	69		81.3		143	233	84	02/10/2015	
	HF3	HF	14.5	98.81	53.52	45.29	73.85	53.21		72.12	67.41		42		90	01/29/2015	
			15.5	90.69	52.5	38.19	64.29	52.81		61.66	63.98		89	339	72	01/29/2015	
			17.85	80.02	42	38.02	61	50.89		59.8	62.5		85	355	75	01/29/2015	
			19.8	91.4	47	44.4	69.5	53.21		64.12	59.05		74	354	30	01/29/2015	
		HTPF	21.25		64.99		74.5	44.96	66.8		58.5	55.07	237	327	45	01/29/2015	
			22.2		57.76		69.5	61.95	68.1		64.27	45	183	93	65	01/29/2015	
		HF	23.5	98.24	53.47	44.77	68.4	62		67.2		68.74	112	202	86	01/28/2015	
		HTPF	25.5		49.01		74.6	49.47	65		45	40	152	242	83	01/28/2015	
		HF	27	81	34	47	67.9	59		66.1	68		35	305	75	01/28/2015	
		HTPF	30.6		67.75		64.88	51.68	59.2		72.41	70.12	129	219	58	01/28/2015	
			31.75		33.2		71.23	62.27	65.8		71.42	71.3	133	223	82	01/27/2015	
		HF	33.1	102.9	59	43.86	72.5	65		69	72		144		90	01/27/2015	

Furthermore, the length of each hydraulic test zone is 3 m, i.e. 2 m for the straddle packer and 1 m for the test chamber, in which 10 tests chamber of HF tests including HF1-33.5, HF2-32.2, HF2-10.4, HF3-31.75, HF3-30.6, HF3-22.2, HF3-21.25, HF3-19.8, HF3-14.5, and AP2-54 have partially overlapped with the adjacent test zone. It means that the rock mass of the test chamber was previously affected by the straddle packer of the previous test. Further studies disclosed that, except for HF3-14.5, it is not a clear contradiction between the key pressure values of each test with the adjacent test. The mentioned procedures have changed four HF tests, i.e. HF3-22, HF 3-31.75, HF 2-21.4, and HF 2-32, to the HTPF tests. It is noticeable that the dip and dip direction of the crack in the mention tests are different from the dip and dip direction of fracture in the previous test.

The artesian circumstance that occurred at a depth from 27 m to 45 m of HF borehole series has three effects: (a) the shut-in pressure in the step rate stage was increased; thus this data was omitted in the stress data analysis, (b) it seems that the rock mass saturation and artesian water pressure made resistance to pressure descending in the borehole test chamber after closing the water injection pipe valve, even up to 3 h; and (c) increasing the water pressure after the test period, which was confined under the straddle packer, would have rapidly pushed out the borehole test apparatuses if the packer pressure had been released similar to the normal situation. Besides, the AP2 tests were conducted at different elevation levels and a limited number of tests compared to the HF series (Tables 1 and 3). Therefore, the data analysis of stress tensor at the

complex caverns elevation utilizes only the HF series information, presented in Sec. 6.

6. Data analysis

The test data was analyzed by the classic (Hubbert and Willis, 1957) [20] and the inversion methods (Hubbert and Willis, 1957; Cornet, 1986) [20; 8]. In the classic method, the fracture dip must be equal to or greater than 75 degrees, and in the inversion method, the joints or cracks must be in diverse ranges. The 20 and 18 test results were selected for the data analysis in the classic (Table 4) and the inversion (Table 5) methods, respectively.

Table 4. HF/HTPF test data utilized in the classic method (GK, 2015) [12].

Phase	Borehole (m)	Test type	Test depth (m)	Fracture strike	Dip	Stage	S(bar)		
							SV	Sh	SH
Second	HF1	HF	27.2	144	90	3	131	51.3	129
			30.8	62	74		132	56.9	144
			33.5	357	75		133	78.8	163
		HTPF	59.5	262	79		140	(54.4)	(98.6)
			63.5	19	90		141	(65.0)	(127.0)
			65.5	61	79		141	(76.4)	(156.0)
			67.5	302	81		142	(73.4)	(154.0)
	HF2	HF	8.4	55	78.5	4	121	65.0	152
		HTPF	10.4	147	72.5		122	(49.8)	(115)
		HF	11.9	133	90		122	61.1	152
		HTPF	28.15	82	75		126	(80.0)	(198)
			32.2	233	79		127	(55.8)	(131)
		HF	33.2	143	84		128	69.0	134
	HF3	HF	14.5	42	90		128	72.1	163
			15.5	89	72		128	61.7	132
			17.85	85	75		128	59.8	137
			23.5	112	86		130	67.2	148
		HTPF	25.5	152	83		130	(65.0)	(146)
		HF	27	35	75		131	68.0	170
		HTPF	31.75	133	82		132	(65.8)	(164)

Table 5. HF/HTPF test data used in the inversion method (GK, 2015) [12].

Phase	Borehole (m)	Test type	Test's depth (m)	Fracture strike	Dip	Test stage	Psi(bar)	
							1 refrac	3 refrac
Second	HF1	HF	27.2	144	90	3		51.3
			30.8	62	74			56.9
			33.5	357	75			78.8
			35.2					75.1
		HTPF	59.5	262	79		54.4	
			65.5	61	79			76.4
			67.5	302	81		73.4	
	HF2	HF	8.4	55	79	4		65.0
		HTPF	10.4	147	73		49.8	
		HF	11.9	133	90			61.1
			28.2	82	75		80	
	HF3	HTPF	15.5	89	72			61.7
			17.9	85	75			59.8
			19.8	74	30			64.1
			23.5	112	86			67.2
		HF	27	35	75		66.1	
		HTPF	31.8	133	82		65.8	
		HF	33.1	144	90			69

6.1. The Sh trend

The correlation between Sh and the depth of the HF/HTPF tests was conducted by the inversion method (Table 6). It should be noted that in the mentioned correlation, the total amount of overburden (z) was the sum of the test depth (Table 5) and borehole overburden (see Table 2). The trend of Sh versus the test's depth in the classic and inversion methods is shown in Figure 12.

Table 6. Sh by the inversion method (GK, 2015) [12].

Boreholes	Test depth (m)	SH (bar)
HF1, HF2, and HF3	8.4 to 67.5	Sh=49.29+0.27(z-468)

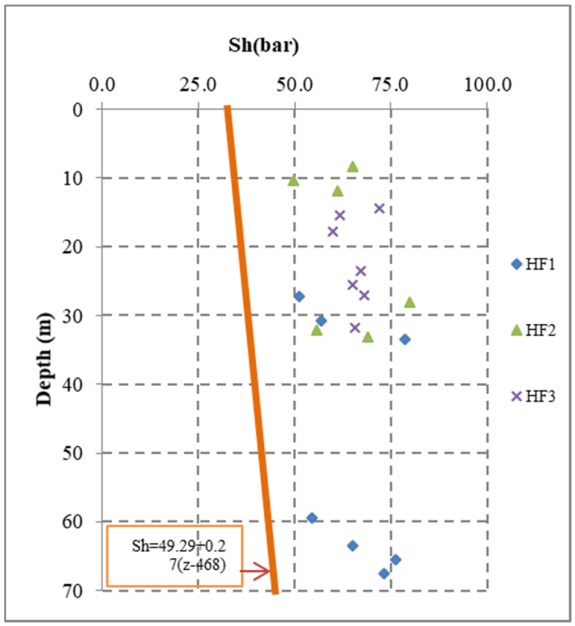

Figure 12. The Sh *vs.* borehole depth in the classic data points and inversion trend line (GK, 2015) [12].

The main points achieved from Figure 12 are as follow:

- The Sh values obtained by each method have a relatively good compatibility.
- The Sh values obtained from each method virtually increase compared to the depth.

6.2. SH trend and azimuth

The correlation of SH and the depth of the HF/HTPF tests was conducted by the inversion method (Table 7). Figure 13 shows the trend of SH versus test depth by the classic and inversion methods, in which:

- In the inversion method, the SH value obtained is less than the relevant magnitude in the classic method.
- The SH values obtained by the classic and inversion methods slightly increased versus the test depth. However, the inversion method shows a higher increasing rate.

Table 7. SH correlation *vs.* test depth by the inversion method (GK, 2015) [12].

Boreholes	Test depth (m)	SH (bar)
HF1, HF2, and HF3	8.4 to 67.5	SH=54.07+0.75(z-468)

According to the second phase of the HF tests, the hydraulic fracture dip/dip direction is indicated in an ENEW-SW direction by the classic method (Figure 14), which is generally adapted with the inversion method azimuths (Table 8).

The SH azimuth has compatibility with the World Stress Map, as shown in Figure 15.

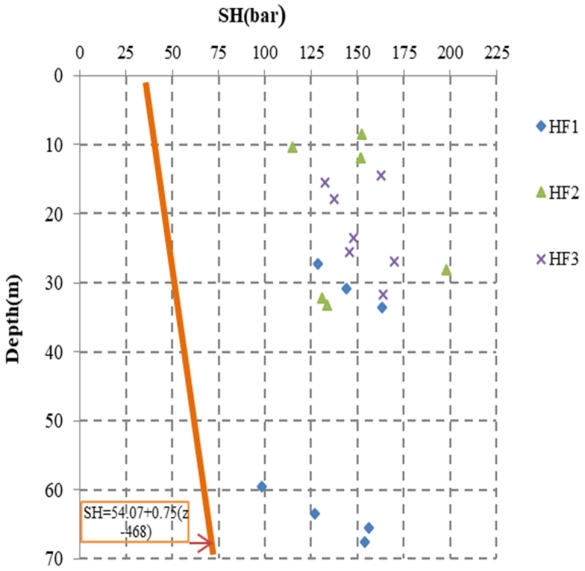

Figure 13. SH *vs.* borehole depth in the classic data points and inversion trend line (GK, 2015) [12].

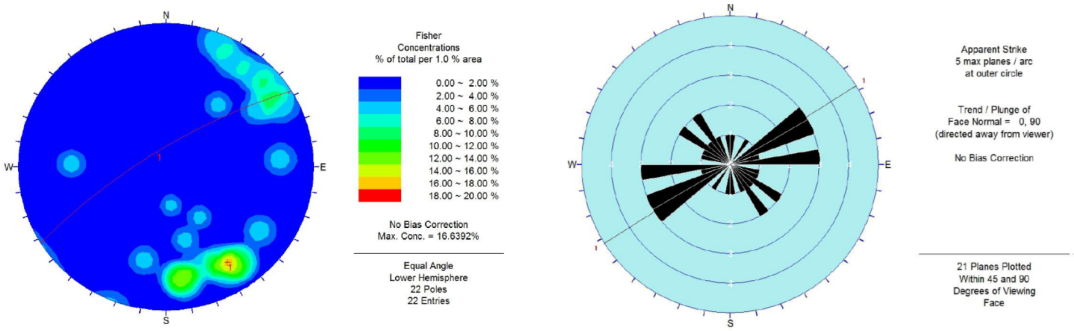

Figure 14. Distribution of hydraulic fractures. Right: pole plot; Left: Rosette plot (*RMRA*, 2013) [33].

Table 8. SH azimuth in the classic and inversion methods (GK, 2015) [12].

Boreholes	Inversion method (degree)	Classic method (degree)
HF1, HF2, and HF3	79 to 89 or ENE-WSW	56 to 93 or ENE-WSW

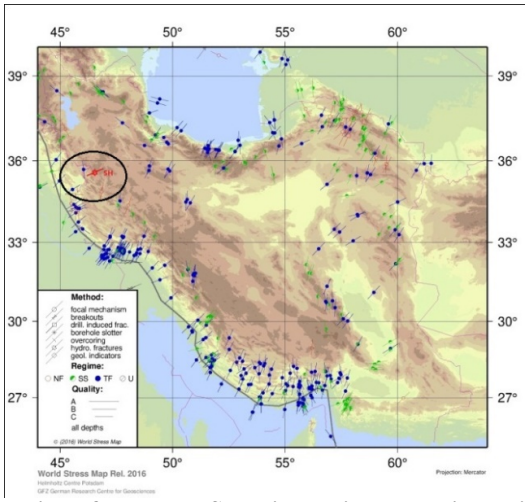

Figure 15. Schematic representation of the mean SH azimuth in comparison with the global focal mechanism directions regime, Iran (WSM 2016-CASMO) [44].

7. Fault slip analysis

The stress elements in the classic method represent strike-slip faulting with the strike of (ENE-WSW), whereas the inversion method represents normal faulting, as shown in Figure 16.

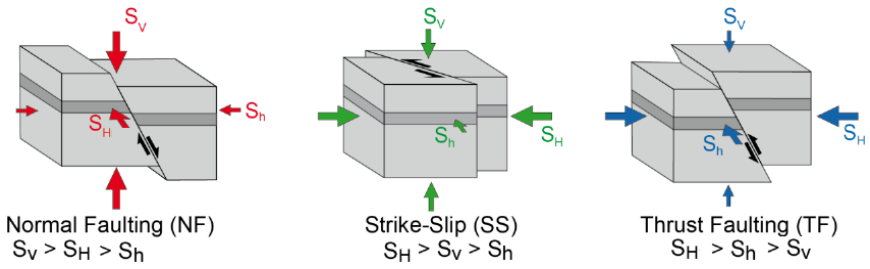

Figure 16. Effects of three main tectonic stress regimes on the faulting type (Oliver Heidbach, 2016) [37].

The main faults analysis (Haimson *et al*. 2003) [17] was performed in the project area in order to identify the correct type of the local stress regime. There were two clockwise strike-slip faults, i.e. Sarvabad and Gorgine, at a distance of 14 km and 6 km, respectively. The project area's geological data and faulting plan were relatively confirmed with the SH azimuth in the classic method. Moreover, the ground surface investigation and major/minor fault analysis at the project area distinguished that the main horizontal stress was azimuth is between N12W; and N38E, the bedding dip/dip directions were (75~80 degrees) and (15~40), respectively. It is noticeable that from the ground surface to the cavern complex level, the variation in the dip direction was about 25 degrees, which may leads to a complicated horizontal stress regime that affect rock mass for a long time.

8. Conclusions

In the previous sections, the relevant HF/HTPF test data in the meta-sandstone with about 10% inter-layer phyllite in the complex rock caverns was reviewed. Despite all the simplified hypotheses in the HF/HTPF theory, i.e. isotropic, elastic, homogeneous, and impermeable rock material, and so on, the HF/HTPF tests are the conventional and practical techniques for the in-situ stress measurement in the hydropower rock caverns. The acceptability and consistency of the HF/HTPF tests depend on several factors such as the rock mass characteristics, borehole drilling type, optimum number of tests, geological information, and relevant geotechnical analysis. The mentioned hydraulic tests measured the magnitudes and azimuths of the principal horizontal stresses. The main achievements of the 37 HF/HTPF tests in the Azad PSPP are as follow:

1. The measured SH and Sh were 7-17 MPa and 4-11 MPa, respectively; the calculated SV was 6-14 MPa at different test locations.
2. The SH azimuth based on the HF and HTPF tests was SW-NE (56-93 degrees) and ENE-WSW (79-89 degrees), respectively, and the mentioned azimuth according to the geological data and fault slip analysis was N12W-N38E.
3. The TV imaginary system has a complementary role in checking the borehole situations, especially in long boreholes.
4. The estimated values for Sh and SH in the classical method are higher than the inversion method. Besides, the classic method is a consistent in-stress regime with the fault slip analysis (SH > Sv > Sh).
5. The inter-layer of the soft rock and the joined discontinuity as a rock mass heterogeneity and the artesian groundwater situation considerably influenced the HF/HTPF tests. The heterogeneity not only in data scattering but also in borehole instability in the long borehole has an undeniable role.

Acknowledgements

The authors would like to show their gratitude to the Iran Water and Power Resources Development Company (IWPC) and Mahab Ghodss Consulting Engineering Company for the use geo-mechanical data of the mentioned hydropower projects.

References

[1]. Abdollahipour, A., Fatehi, M.M., Yarahmadi, B.A. and Gholamnejad, J. (2016). Numerical investigation of effect of crack geometrical parameters on hydraulic

fracturing process of hydrocarbon reservoirs. Journal of Mining and Environment, Vol.7, No.2, 2016, 205-214.

[2]. Amadei, B., and Stephansson, O. (1997). Rock stress and its measurement. Springer Science and Business Media.

[3]. Alemdag, S., Zeybek, H.I., and Kulekci, G. (2019). Stability evaluation of the Gümüşhane-Akçakale cave by numerical analysis method. Journal of Mountain Science. 16 (9): 2150-2158.

[4]. ASTM D 4645 2008. Standard Test Method for Determination of In-Situ Stress in Rock Using Hydraulic Fracturing Method, American Society for Testing and Materials, West Conshohocken, Philadelphia, PA.

[5]. Bakhshi, E., Rasouli, V., Ghorbani, A., Marji, M.F., Damjanac, B. and Wan, X. (2019). Lattice numerical simulations of lab-scale hydraulic fracture and natural interface interaction. Rock Mechanics and Rock Engineering. 52 (5): 1315-1337.

[6]. Bai, X., Zhang, D.M., Wang, H., Li, S.J. and Rao, Z. (2018). A novel in situ stress measurement method based on acoustic emission Kaiser effect: a theoretical and experimental study. Royal Society open science. 5 (10): 181263.

[7]. Cornet, F.H. and Valette, B. (1984). In situ stress determination from hydraulic injection test data. Journal of Geophysical Research: Solid Earth. 89 (B13): 11527-11537.

[8]. Cornet, F.H. (1986, August). Stress determination from hydraulic tests on preexisting fractures-the

HTPF method. In ISRM International Symposium. OnePetro.

[9]. Cornet, F.H. (1993). The HTPF and the integrated stress determination methods. In Rock testing and site characterization (pp. 413-432). Pergamon.

[10]. Cornet, F.H., Li, L., Hulin, J.P., Ippolito, I., and Kurowski, P. (2003). The hydro-mechanical behavior of a fracture: an in situ experimental case study. International Journal of Rock Mechanics and Mining Sciences. 40 (7-8): 1257-1270.

[11]. Feng, Yu. Harrison, John P. and Bozorgzadeh, N. 2019. Uncertainty in In-situ Stress Estimations: A Statistical Simulation to Study the Effect of Numbers of Stress Measurements, Rock Mechanics and Rock Engineering 52, pages 5071–5084.

[12]. GK-Gamaneh Kav Co. 2015. Azad PSPP final report of hydraulic fracturing.

[13]. Gaines, S., Diederichs, M.S. and Hutchinson, D.J. (2012). Review of borehole in situ stress measurement techniques for various ground conditions and numerical stress estimation considerations. In 46th US Rock Mechanics/Geomechanics Symposium. American Rock Mechanics Association.

[14]. Haimson, B. and Fairhurst, C. (1970). Hydraulic fracturing in porous-permeable materials. Journal of Petroleum Technology. 21 (07): 811-817.

[15]. Haimson, B. and Fairhurst, C. (1969). In-situ stress determination at great depth by means of hydraulic fracturing. In The 11th US symposium on rock mechanics (USRMS). American Rock Mechanics Association.

[16]. Haimson, B.C. 1989. Hydraulic fracturing stress measurements, special issue, Int. J. Rock Mech. Min. Sci. Geomech. Abstr. 26: 447–685.

[17]. Haimson, B.C., and Cornet, F.H. 2003, ISRM suggested methods for rock stress estimation—part 3: hydraulic fracturing (HF) and/or hydraulic testing of pre-existing fractures (HTPF). International Journal of Rock Mechanics and Mining Sciences. 40 (7-8): 1011-1020.

[18]. Haimson, B.C. and Lee, M. Y. (1984). Development of a wireline hydro-fracturing technique and its use at a site of induced seismicity. In The 25th US Symposium on Rock Mechanics (USRMS). American Rock Mechanics Association.

[19]. Huan, X., Xu, G., Zhang, Y., Sun, F. and Xue, S. (2021). Study on Thermo-Hydro-Mechanical Coupling and the Stability of a Geothermal Wellbore Structure. Energies. 14 (3): 649.

[20]. Hubbert, M.K. and Willis, D.G. (1957). Mechanics of hydraulic fracturing. Transactions of the AIME. 210 (01): 153-168.

[21]. Hudson, J.A., Cornet, F.H. and Christiansson, R. (2003). ISRM Suggested Methods for rock stress Estimation-Part 1: Strategy for rock stress estimation. International Journal of Rock Mechanics and Mining Sciences. 40 (7-8): 991-998.

[22]. Hudson, A. 1995. Comprehensive rock engineering- Rock Testing and Site Characterization-Principles, Practice and Projects, chapter 15, page: 413-431.

[23]. Hung, J.H., Ma, K.F., Wang, C.Y., Ito, H., Lin, W. and Yeh, E.C. (2009). Subsurface structure, physical properties, fault-zone characteristics and stress state in scientific drill holes of Taiwan Chelungpu Fault Drilling Project. Tectonophysics. 466 (3-4): 307-321.

[24]. Ji, M. and Guo, H. (2020). Influence of in-situ rock stress on the stability of roadway surrounding rock: a case study. Journal of Geophysics and Engineering. 17 (1): 138-147.

[25]. Kehle, R.O. (1964). The determination of tectonic stresses through analysis of hydraulic well fracturing. Journal of Geophysical Research. 69 (2): 259-273.

[26]. Kim, K. and Franklin, J. (1987). Suggested methods for rock stress determination. In International

Journal of Rock Mechanics and Mining Sciences & Geomechanics Abstracts (Vol. 24, No. 1, pp. 53-73.

[27]. Krietsch, H., Gischig, V., Jalali, M.R., Amann, F., Evans, K.F., Doetsch, J. and Valley, B. (2017). Stress measurements in crystalline rock: Comparison of overcoring, hydraulic fracturing and induced seismicity results. In 51st US Rock Mechanics/Geomechanics Symposium. American Rock Mechanics Association.

[28]. Lakirouhani, A., Detournay, E., and Bunger, A.P. (2016). A reassessment of in situ stress determination by hydraulic fracturing. Geophysical Journal International. 205 (3): 1859-1873.

[29]. Lan, Q., Zhen-hua, X., Kui, Z., Yuan, L., Yang, L., Ke-jia, W., and Hui, C. (2011). Study on acoustic emission in-situ stress measurement techniques based on plane stress condition. Procedia Engineering. 26: 1473-1481.

[30]. Li, H., Lin, B., Hong, Y., Gao, Y., Yang, W., Liu, T. and Huang, Z. (2017). Effects of in-situ stress on the stability of a roadway excavated through a coal seam. International Journal of Mining Science and Technology. 27 (6): 917-927.

[31]. Liu, Q., Sun, L., and Tang, X. (2019). Investigate of the influence of the in-situ stress conditions on the grout penetration process in fractured rocks using the combined finite-discrete element method. Engineering Analysis with Boundary Elements. 106: 86-101.

[32]. Ljunggren, C., Chang, Y., Janson, T. and Christiansson, R. (2003). An overview of rock stress measurement methods. International Journal of Rock Mechanics and Mining Sciences. 40 (7-8): 975-989.

[33]. Mahab Ghoods Co. 2013. RMRA-Rock Mechanics Report of Azad PSPP, Phase II.

[34]. Mahab Ghoods Co. 2013. EGRA-Engineering Geology Report of Azad PSPP, Phase II.

[35]. Miao, S.J., Cai, M.F., Guo, Q.F., and Huang, Z.J. (2016). Rock burst prediction based on in-situ stress and energy accumulation theory. International Journal of Rock Mechanics and Mining Sciences. 100 (83): 86-94.

[36]. Mortimer, L., Aydin, A., Simmons, C.T., Heinson, G., and Love, A.J. (2011). The role of in situ stress in determining hydraulic connectivity in a fractured rock aquifer (Australia). Hydrogeology Journal. 19 (7): 1293-1312.

[37]. Oliver Heidbach 2016. WSM Scientific Technical Report 16-01.

[38]. Rutqvist, J., Tsang, C. F. and Stephansson, O. (2000). Uncertainty in the maximum principal stress estimated from hydraulic fracturing measurements due to the presence of the induced fracture. International Journal of Rock Mechanics and Mining Sciences. 37 (1-2): 107-120.

[39]. Sano, O., Ito, H., Hirata, A. and Mizuta, Y. (2005). Review of methods of measuring stress and its variations. Bull. Earthq. Res. Inst. Univ. Tokyo, 80, 87-103.

[40]. Serata, S., Sakuma, S., Kikuchi, S. and Mizuta, Y. (1992). Double fracture method of in situ stress measurement in brittle rock. Rock mechanics and rock engineering. 25 (2): 89-108.

[41]. Scheidegger, A.E. (1960). On the connection between tectonic stresses and well fracturing data. Geofisica pura e applicate. 46 (1): 66-76.

[42]. Shahverdiloo, M.R. (2010). Estimation of minimum in situ stress by hydrojacking method case study of Siah bisheh power plant. In ISRM International Symposium on In-Situ Rock Stress. OnePetro.

[43]. Shahverdiloo, M.R., Behnia, M., Anvari, A. and Motlagh, M.A. (2014). Revise of cavern's axis azimuth in Azad pumped storage project. In ISRM Regional Symposium-EUROCK 2014. International Society for Rock Mechanics and Rock Engineering.

[44]. WSM 2016-CASMO - Create a Stress Map Online, Iran Stress Map, Available from: http://www.world-stress- map.org/casmo/ [Accessed on 14 March 2020].

[45]. Xiao, Y.X., Feng, X.T., Hudson, J.A., Chen, B.R., Feng, G.L. and Liu, J.P. (2016). ISRM suggested method for in-situ microseismic monitoring of the fracturing process in rock masses. Rock Mechanics and Rock Engineering. 49 (1): 343-369.

[46]. Zang, A. and Stephansson, O. (2009). Stress field of the Earth's crust. Springer Science and Business Media.

[47]. Zoback, M.D. and Haimson, B.C. (1982). Status of the hydraulic fracturing method for in-situ stress measurements. In The 23rd US Symposium on Rock Mechanics (USRMS). American Rock Mechanics Association.

چالش‌های اندازه‌گیری تنش برجا در مغارهای سنگی با آزمایش‌های شکست هیدرولیکی و HTPF- مطالعه موردی طرح نیروگاه برق‌آبی آزاد

محمدرضا شاهوردیلو* و شکراله زارع

دانشکده مهندسی معدن، نفت و ژئوفیزیک، دانشگاه صنعتی شاهرود، شاهرود، ایران

ارسال ۲۰۲۱/۰۴/۱۸، پذیرش ۲۰۲۱/۰۶/۰۷

* نویسنده مسئول مکاتبات: mr.shahverdiloo@shahroodut.ac.ir

چکیده:

شکست هیدرولیکی (HF) و آزمایش هیدرولیکی شکستگی‌های قبلی (HTPF) روش‌های هیدرولیکی موثری برای تعیین تنش برجا در توده‌سنگ می‌باشند. معمولا، تنش اصلی برجای افقی حداقل (Sh) و حداکثر (SH) با روش‌های هیدرولیکی اندازه‌گیری شده و تنش قائم (SV) با استفاده از وزن لایه‌های روباره سنگی محاسبه می‌شوند. این مقاله بر اجرای ۳۷ آزمایش HF و HTPF در ماسه‌سنگ دگرگونی با حدود ۱۰ درصد میان‌لایه فیلیتی تمرکز دارد. از مهمترین چالش‌های و محدودیت‌های مطرح در آزمایش‌های اشاره شده می‌توان به وجود شرایط آرتزین در برخی گمانه‌ها، فاصله زمانی زیاد بین حفاری و آزمایش هیدرولیک در گمانه‌های بلند، عدم دسترسی به سازه‌های زیرزمینی اصلی مغارها در دوره زمانی ابتدای پروژه و فرضیات ساده‌سازی شده تئوریک در محاسبات آزمایش HF/HTPF می‌باشند. بدلیل ناپایداری در دیواره گمانه‌های بلند نسبت به بازنگری درنوع دستگاه حفاری و طول گمانه اقدام و همچنین استفاده از دوربین درون گمانه‌ای در فرآیند انتخاب عمق آزمایش الزامی شد. به منظور بهینه‌سازی تعداد آزمایش‌ها مرحله به مرحله داده‌های آزمایش‌های HF/HTPF با روش کلاسیک و اینورژن مورد تجریه و تحلیل قرار گرفت. مقدار SH در روش تحلیل اینورژن کمتر از مقدار روش کلاسیک بدست آمد. با استفاده از روش آنالیز صفحه گسل و سایر داده‌های زمین‌شناسی منطقه، مقدار و جهات تنش‌های اصلی با روش کلاسیک معتبر شناخته شد. مقدار تنش بیشینه و کمینه افقی در محل آزمایش‌ها به ترتیب ۷-۱۷ مگاپاسکال و ۴-۱۱ مگاپاسکال بدست آمد و مقدار محاسبه و برای تنش قائم نیز در بازه ۶-۱۱ مگاپاسکال قرار گرفت. در حقیقت رژیم تنش منطقه به صورت $SH > SV > Sh$ و راستای تنش افقی بیشینه در بازه ۵۶-۹۳ درجه تعیین شد.

کلمات کلیدی: اندازه‌گیری تنش، رژیم تنش، شکست هیدرولیکی، HTPF، ناهمگنی.